Progress in Oceanography 239 (2025) 103581

Contents lists available at ScienceDirect

Progress in Oceanography

journal homepage: www.elsevier.com/locate/pocean

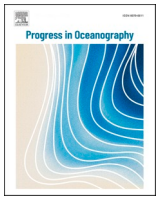

Environmental drivers of foraging by deep-diving cetaceans: Roles of mesoscale oceanography and light-driven cycles

Thomas A. Clay [a,b,c,*], Gemma Carroll [a,b,c], Megan A. Cimino [a,b], Jennifer L. Miksis-Olds [d], Katie A. Kowarski [e], Anthony P. Lyons [d,f], Peter I. Miller [g], Timothy S. Moore [h], Joseph D. Warren [i], Elliott L. Hazen [a,b]

[a] Institute of Marine Sciences, University of California, Santa Cruz, Santa Cruz, CA, USA
[b] Southwest Fisheries Science Center, Ecosystem Science Division, National Oceanic and Atmospheric Administration (NOAA), Monterey, CA, USA
[c] Environmental Defense Fund, San Francisco, CA, USA
[d] Center for Acoustics Research and Education, University of New Hampshire, Durham, NH, USA
[e] JASCO Applied Sciences, Dartmouth, NS, Canada
[f] Center for Coastal and Ocean Mapping, University of New Hampshire, Durham, NH, USA
[g] Remote Sensing Group, Plymouth Marine Laboratory, Plymouth, UK
[h] Harbor Branch Oceanographic Institute, Florida Atlantic University, Fort Pierce, FL, USA
[i] School of Marine and Atmospheric Sciences, Stony Brook University, Southampton, NY, USA

ARTICLE INFO

Keywords:
Beaked whale
Eddies
Gulf Stream
Habitat
Kogia
Lunar cycle
Passive acoustic monitoring

ABSTRACT

Foraging by deep-diving marine predators is shaped by the interplay between oceanographic features and light-driven (diel and lunar) cycles that structure the three-dimensional distributions of their mesopelagic prey. While mesoscale features such as fronts and eddies are important for epipelagic predators, their role in driving the foraging behaviour of deep-divers remains poorly understood. We investigated bio-physical drivers of habitat use for dwarf and pygmy sperm whales *Kogia* spp. and beaked whales *Mesoplodon* spp. using three years of passive acoustic monitoring at seven sites on the Outer Continental Shelf of the northwest Atlantic Ocean. We analysed acoustic detections alongside satellite- and model-derived oceanographic variables spanning meso- and seasonal scales, and diel and lunar cycles. The two deepest sites, on the Blake Plateau (870 m) and the outer continental slope (790 m), emerged as foraging hotspots with year-round vocal presence of kogiid and beaked whales. Mesoscale activity associated with the Gulf Stream – including current strength and eddy kinetic energy – were foraging predictors, alongside sea surface temperature and primary productivity. However, site-specific habitat models explained only 3–37 % deviance. Blainville's beaked whale *M. densirostris* foraging activity peaked during the full moon, likely due to lunar effects on prey concentrations at depth, while there was no clear diel variation for any detected beaked whale species. In contrast, kogiid foraging activity was elevated around sunrise and sunset. These findings suggest a role of near-surface features such as eddies in addition to light-driven cycles in shaping predator–prey dynamics, even in deep continental slope ecosystems.

1. Introduction

Marine predators move to track the dynamic distribution of their preferred habitats and prey across four dimensions (longitude, latitude, depth and time; Benoit-Bird et al. 2019; Braun et al., 2023; Carroll et al., 2021). Over large-scales, animals may conduct seasonal, long-distance migrations to follow predictable variations in ocean temperature and productivity (Block et al., 2011). Over finer spatiotemporal scales, predators navigate a dynamic seascape structured by bio-physical gradients that influence predator–prey interactions and predator foraging success (Abrahms et al., 2018; Sabarros et al., 2009). For deep-diving predators, tracking prey within the mesopelagic "twilight zone" (200–1000 m) requires responding to both the vertical movements of micronekton and the dynamic oceanographic features that aggregate and concentrate these prey layers (Braun et al., 2022). Light — through diel and lunar cycles — also acts as a primary cue organizing predator–prey interactions, influencing the daily vertical migrations of micronekton and predator foraging behaviour (Benoit-Bird et al., 2009;

* Corresponding author.
E-mail address: tommy.clay@outlook.com (T.A. Clay).

https://doi.org/10.1016/j.pocean.2025.103581
Received 4 November 2024; Received in revised form 19 September 2025; Accepted 25 September 2025
Available online 5 October 2025

Owen et al., 2019). The interplay between physical oceanography and light-driven vertical structuring of prey likely governs the habitat use and foraging behaviour of deep-diving species yet remains poorly understood.

Mesoscale (10–100 km) and sub-mesoscale (1–10 km) features like fronts, eddies and meanders, create horizontal and vertical gradients in temperature, salinity and density, that often enhance nutrient retention and primary productivity (Chelton et al., 2011; Mahadevan, 2019). These features physically aggregate plankton (e.g. Mullaney and Suthers, 2013), creating foraging "hotspots" that attract upper-trophic level consumers (e.g. Arostegui et al., 2022; Kai et al., 2009). While marine predators' associations with eddies and fronts is well-established (e.g. Abrahms et al., 2018; Bailleul et al., 2010; Scales et al., 2014a; Scales et al., 2014b), their role in deep-diving predator foraging is less clear (Braun et al., 2022). Mesoscale features likely connect surface and subsurface processes, facilitating deep-diving predator foraging through multiple pathways. For example, eddies can increase mesopelagic micronekton biomass (Della Penna and Gaube, 2020) and create thermal corridors for diving predators to access deeper waters (Arostegui et al., 2022; Braun et al., 2019). Fronts may aggregate mesopelagic communities nearer the surface, increasing accessibility to air-breathing predators (Rivière et al., 2019). Additionally, eddies and fronts may create foraging opportunities by downwelling nutrients and attracting micronekton, or by deepening the thermocline, which compresses prey within the deep-scattering layer (Acha et al., 2015; Arostegui et al., 2022; Lévy et al., 2018; Wang et al., 2024).

Deep-diving cetaceans, including pygmy and dwarf sperm whales (Kogiidae) and beaked whales (Ziphiidae), are oceanic predators that conduct long dives (up to 222 min) to hunt fish and cephalopods in meso- to bathypelagic waters (200–3000 m; Quick et al., 2020; Schorr et al., 2014; Shearer et al., 2019). They are globally distributed, but challenging to study due to their offshore distributions, brief surface intervals, and for some species, their inconspicuous surfacing behaviour (Hodge et al., 2018; Hooker et al., 2019). Knowledge of their habitat requirements mostly comes from ship-based visual surveys, which cover broad areas but are limited to short durations (days to months), daylight and good weather (Roberts et al., 2016). Biologging has advanced understanding of their distribution and diving behaviour (e.g. Shearer et al., 2019; Tyack et al., 2006; Visser et al., 2021), however tags are difficult to attach and provide data for only up to a few months. Because toothed whales use biosonar clicks to locate prey (Johnson et al., 2004), their foraging behaviour can be monitored using seafloor-mounted or drifting hydrophones, enabling continuous, long-term and high-resolution sampling at the population and community level (Fregosi et al., 2020; McCullough et al., 2021). An increasing number of multi-year acoustic studies have revealed temporal patterns in the occurrence and foraging behaviour of deep-diving whales across broad spatial and temporal (from hours to years) scales (e.g. Cohen et al., 2023; Hodge et al., 2018; Kowarski et al., 2018, 2023; Stanistreet et al., 2017).

Light strongly influences prey distribution in the twilight zone, and diel (day-night) and lunar cycles thereby influence deep-diving cetacean foraging behaviour, though effects vary across species and depth guilds (e.g., Hazen and Johnston, 2010, Urmy and Benoit-Bird, 2021). Studies have shown that species targeting mesopelagic fish and squid, such as short-finned pilot whales *Globicephala macrorhynchus*, common dolphins *Delphinus delphis* and Risso's dolphins *Grampus griseus*, modulate their foraging and dive behaviour according to lunar and diel cycles; the former two species have deeper and longer dives or reduced echolocation during the full moon (Cohen et al., 2023; Owen et al., 2019; Simonis et al., 2017), while the latter two primarily show nocturnal or crepuscular foraging, with Risso's dolphins diving deeper during the day (>400 m; Benoit-Bird et al., 2019, Cohen et al., 2023, Visser et al., 2021), These cyclical patterns most likely reflect the vertical migration of micronekton, which concentrate nearer the surface at night and during the new moon (Benoit-Bird et al., 2019). In contrast, deep-diving beaked whales reduce foraging dives (>~500 m, generally around 800–2000 m) at night and spend more time resting near the surface, likely because this is when visual predators such as killer whales *Orcinus orca* are less active (Baird et al. 2006; Barlow et al., 2020; Schorr et al., 2014). However, goose-beaked (previously Cuvier's; Rogers et al., 2024) whales *Ziphius cavirostris* show no diel variation in dive depth (>800 m; Shearer et al., 2019), suggesting they target deep-scattering layers of benthopelagic prey with weak vertical migration (Arranz et al., 2011). Kogiid whales remain poorly understood and there are no data on foraging dive depths, however studies of the diets of stranded animals suggest they predominantly target cephalopods, and to a lesser extent fish, in the epi- and mesopelagic (up to 1000 m) (Beatson, 2007; West et al., 2009). Additionally, passive acoustic studies indicate a general pattern of diurnal activity which could reflect deeper diving behaviour near bottom-mounted hydrophones (Hildebrand et al., 2019; Ziegenhorn et al., 2023).

In this study, we used passive acoustic monitoring to assess the extent to which near-surface oceanographic features and diel and lunar cycles influence the foraging activity of beaked and kogiid whales in the north-west Atlantic. The region is highly dynamic, with complex bathymetry and oceanography, supporting high cetacean biodiversity (e.g. Roberts et al., 2016; Virgili et al., 2019, Kowarski et al. 2023). The north-west Atlantic exhibits strong seasonal variation in sea surface temperature and primary productivity, largely driven by the Gulf Stream, which carries warm, saline water northward along the shelf break of the South-Atlantic Bight until veering east at Cape Hatteras (Fig. 1). As it turns east, the Gulf Stream generates large eddies within the semi-enclosed Mid-Atlantic Bight, attracting diverse top predators (e.g. Braun et al., 2023). Several fronts form along the continental slope, including the Hatteras Front, which marks the boundary between warm Gulf Stream waters to the south and east, and cold, productive sub-polar waters to the north and west (Belkin et al., 2009; Savidge and Austin, 2007). Visual surveys have reported high densities of deep-diving cetaceans in abyssal plains, along steep continental slopes and in submarine canyons, where meso- and benthopelagic prey are concentrated (Arranz et al., 2011; Johnston et al., 2008; Waring et al., 2001), and elevated densities of beaked whales and kogiids *Kogia* spp. have been recorded in regions of moderate to high surface temperature gradients, indicative of frontal zones, and for kogiids, in regions of high eddy activity (Virgili et al., 2019; Waring et al., 2001). Though, acoustic studies suggest these species show less seasonal variation than shallower-diving delphinids (e.g. Cohen et al., 2023), indicating greater residency and weaker responses to seasonal patterns of productivity (Foley et al., 2021; Hodge et al., 2018).

We compared the presence of foraging clicks of two groups of deep-diving whales – kogiid and beaked whales – to those of more shallow-diving delphinids across different habitats and over the annual cycle, building on general patterns of cetacean occurrence previously described using a subset of the data (Kowarski et al., 2023). Daily and hourly click detection rates of deep-diving species were then associated with satellite- and model-derived oceanography and the lunar phase, and time of day, respectively, to examine the relative importance of light (e.g. diel and lunar effects on prey vertical migration depth), seasonal (e.g. SST, productivity) and mesoscale and sub-mesoscale (e.g. fronts, eddies) phenomena, on foraging detections. We hypothesized that measures of frontal and eddy activity could influence the foraging behaviour of deep-diving species through multiple mechanisms (see below). Additionally, given their presumed shallower dive behaviour compared to beaked whales, we predicted greater sensitivity of kogiids to light-driven cycles. Our findings increase understanding of the spatiotemporal drivers of foraging activity of deep-diving cetaceans, including the near-surface environmental features that may indicate enhanced foraging opportunities in the deep ocean.

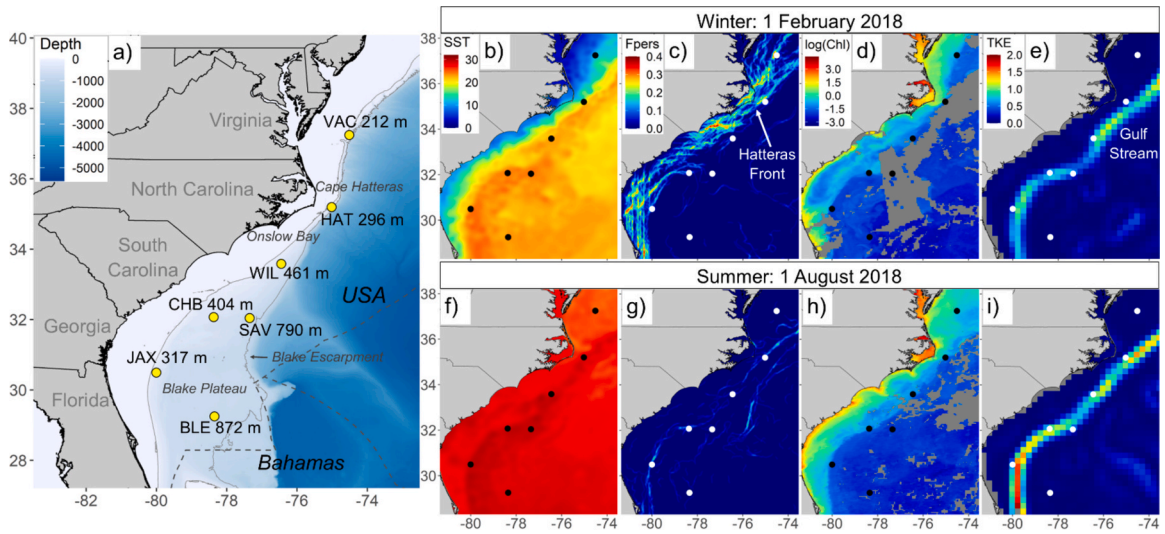

Fig. 1. A) Study region and lander sites along the south-eastern U.S. continental shelf in relation to bathymetry. The locations of lander sites are shown by yellow circles with the depth indicated. Major topographic features are shown in italicised grey text, the 100 and 1,000 m isobaths are shown by solid grey lines and Exclusive Economic Zone boundaries are by dashed grey lines. Maps for a candidate day in b-e) winter and g-i) summer displaying major oceanographic features and seasonal variation for: sea surface temperature (SST, in °C; b, f), front persistence (FPers, value between 0 and 1; c, g), the log of chlorophyll-*a* concentration (log [Chl], mg/m^3; d, h) and total kinetic energy (TKE, in m/s; e, i). The position of the Hatteras Front and Gulf Stream Current are indicated.

2. Methods

2.1. Data collection

Passive acoustic recordings were acquired from seven sites along the southeastern U.S. Outer Continental Shelf across three years, as part of the Atlantic Deepwater Ecosystem Observatory Network (ADEON) project (Miksis-Olds et al., 2025; Table 1): Virginia Inter-Canyon (VAC; 212 m), Hatteras South (HAT; 296 m), Wilmington (WIL; 461 m), Charleston Bump (CHB; 404 m), Savannah Deep (SAV; 790 m), Jacksonville (JAX; 317 m), and Blake Escarpment (BLE; 872 m) (Fig. 1, Table 1). Sites spanned 8° latitude and encompassed a range of sea floor depths from ~ 200 to 900 m. Different oceanographic processes influence each site, with some sites lying in the path of the Gulf Stream, while others are located in regions of elevated frontal and/or eddy activity (Fig. 1). For further details on study design and data collection and processing, see Miksis-Olds et al. (2021), Miksis-Olds et al., (2025) and Kowarski et al. (2023). In summary, Autonomous Multichannel Acoustic Recorders (AMAR, JASCO Applied Sciences) were incorporated into ocean bottom landers and deployed on the seafloor from November–December 2017 to December 2020 (Table 1). AMAR G3 hydrophone systems which sampled at 8 and 375 kHz were used between November 2017 and 2018; thereafter, the next generation AMAR G4 recorders which sampled at 16 and 512 kHz were used. The use of two different frequency bands did not influence detection rates (Kowarski et al., 2023). The higher frequency data (375 and 512 kHz sample rates) were used to identify odontocetes. High frequency data were recorded over duty-cycles which varied according to the AMAR model and recording period, but ranged from 1-min on, 20-min off over a 21-min recording cycle, to 6-min on, 54-min off over a 60-min recording cycle (see Table A1 in Appendix A). Data collection at VAC was contaminated by noise during the first six-month deployment, so data were only usable starting in June 2018. The VAC lander was also prematurely trawled twice which eliminated data from 11 July to 20 October 2019 and from 30 June to 30 November 2020.

2.2. Automated acoustic data processing and species identification

Odontocete clicks, indicators of active foraging, were identified from the high sampling rate (375 and 512 kHz) data using JASCO's custom combined energy detector and classification algorithm (Kowarski et al., 2018). A Teager-Kaiser energy detector was used to identify potential echolocation clicks, and for each detected click, zero-crossing characteristics were calculated and compared to an acoustic library of species-specific odontocete click features. Automatically detected clicks were assigned to the species with the lowest Mahalanobis distance using equivalent library template parameters. Kogiid and beaked whales are distinguishable by the specific characteristics of their vocalizations (see Appendix A, Kowarski et al., 2023 for details). Beaked whales have stereotyped echolocation, and species-specific differences in click characteristics such as upsweeping frequency modulation, peak frequency, spectral content, and inter-click intervals can therefore be used to discriminate four of the six species inhabiting the northwest Atlantic Ocean: northern bottlenose *Hyperoodon ampullatus*, Sowerby's *Mesoplodon bidens*, goose-beaked, and Blainville's *M. densirostris* beaked whales (e.g. Baumann-Pickering et al., 2013; Cohen et al., 2022; Stanistreet et al., 2017). The remaining two species, Gervais' *M. europaeus* and True's *M. mirus* beaked whales, have similar click characteristics

Table 1
Lander site characteristics and total recording durations.

Station name	Abbreviation	Location	Depth (m)	Depth class	Total recording duration (d)
Virginia Inter-Canyon	VAC	37.24°N, 74.51°W	212	Shallow	878.9
Hatteras South	HAT	35.20°N, 75.02°W	296	Shallow	1,098.7
Wilmington	WIL	33.59°N, 76.45°W	461	Intermediate	1,098.3
Charleston Bump	CHB	32.07°N, 78.37°W	404	Intermediate	1,097.4
Savannah Deep	SAV	32.04°N, 77.35°W	790	Deep	1,090.2
Jacksonville	JAX	30.49° N, 80.00°W	317	Shallow	1,051.7
Blake Escarpment	BLE	29.25°N, 78.35°W	872	Deep	1,119.3

which makes distinguishing the two acoustically challenging (DeAngelis et al., 2018); hence, they were considered one acoustic group 'Gervais'/True's' beaked whales. Similarly, both pygmy *K. breviceps* and dwarf sperm whales *K. sima* produce narrow-band high-frequency (NBHF) clicks and cannot be distinguished from each other (Merkens et al., 2018); hereafter they are considered as kogiids. Harbour porpoises *Phocoena phocoena* also use NBHF echolocation but are rarely seen south of Cape Hatteras with the southernmost strandings recorded in Onslow Bay (Hodge et al., 2018) (Fig. 1); as such we were confident that NBHF detections south of the WIL lander were from kogiids and not harbour porpoises (*sensu* Kowarski et al., 2023). Sperm whales *Physeter macrocephalus* were also initially considered and were manually detected at every site (Kowarski et al. 2023); however, given they were infrequently detected and click detector performance was generally low (see below; Table A2), we did not include them in further analyses. Lastly, we also considered unspecified delphinids, which have clicks that are neither frequency modulated like beaked whales, NBHF like kogiids, or with energy below 10 kHz like sperm whales, but which could belong to a range of species (see Appendix A), to contrast seasonal and regional patterns with the deeper-diving species (Fig. 2).

To determine automated detector performance and verify species occurrence, a subset of 0.5 % of acoustic data (corresponding to 71.85 h of 1-min long 375 or 512 kHz data) was visually and aurally reviewed by experienced bio-acousticians using PAMlab (JASCO Applied Sciences). Acoustic data were selected for manual review using the Automated Data Selection for Validation (ADSV) method which automatically selects a semi-random subset of representative data for manual review, which was conducted blind to the results of the automated detector (Kowarski et al., 2021). The presence or absence of identifiable signals of each cetacean species group was calculated, and the automated detector's per file precision (*P*) and recall (*R*) were provided for each station and deployment period, whereby *P* is the proportion of automated detections that are true positives and *R* is the proportion of clicks that are identified by the automated detector (Kowarski et al., 2018; Roch et al., 2011). A cut-off precision score of 0.70 (70 % of 1 min files with automated detections that contain the species detected) was used for inclusion in further analyses, resulting in the removal of one deployment period for Gervais'/True's beaked whales (4.7 % of days) and two for kogiids (17.0 %) (Table A2). By expanding the unit of measure from 1-min acoustic files to 1 h, the automated detector performance increased as there is greater time and opportunity for the automated detector-classifier to identify signals as animals move through the water column (Kowarski et al., 2020). Therefore, the per file automated performance metrics can be considered an underestimate of 1 h detector performance. Hourly presence or absence of a click of each species was recorded and summarized by the number of hours detected per day (detection positive hours [DPH]), which was considered an indicator of daily foraging activity.

2.3. Oceanographic data

All environmental data extraction and statistical analyses were conducted in R *v.* 4.0.3 (R Core Team 2020). Oceanographic variables known to be important for the focal species were selected (Roberts et al.,

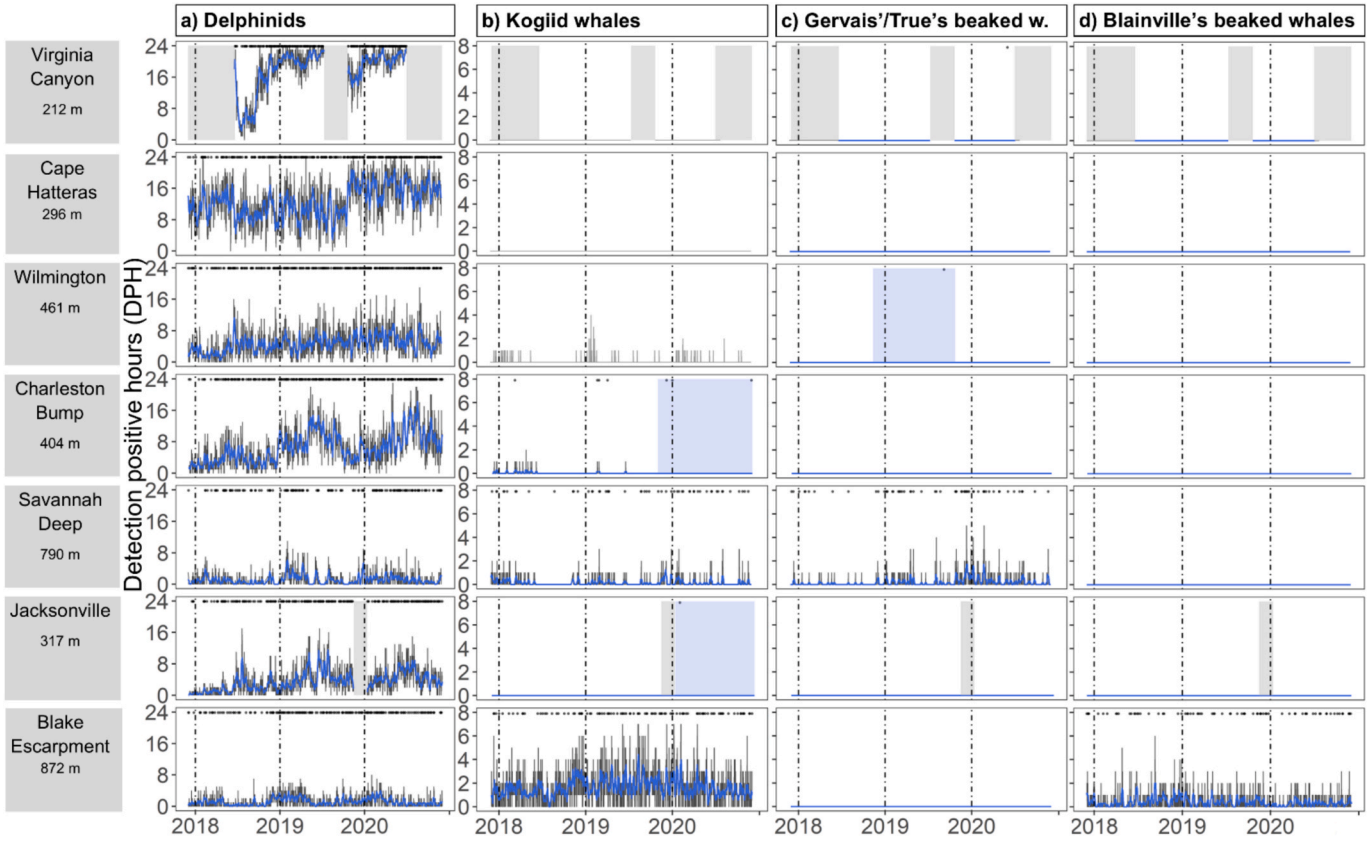

Fig. 2. Time series of daily automated detection positive hours (DPH) for a) unspecified delphinids, b) kogiid whales, c) Gervais'/True's beaked whales, and d) Blainville's beaked whales, from seven lander sites in northwest Atlantic Ocean: Virginia Inter-Canyon (VAC), Hatteras South (HAT), Wilmington (WIL), Charleston Bump (CHB), Savannah Deep (SAV), Jacksonville (JAX), Blake Escarpment (BLE). The depth of the lander is also shown. Raw daily DPH are shown with black lines and the smoothed 7-day running mean is shown with blue lines. Black dots at the top of each plot indicate days for which manually-validated clicks were detected. The grey shaded boxes for VAC and JAX represent periods when data were not collected due to logistical constraints, while blue shaded boxes indicate periods when automated precision was lower than 0.7. Note that the y-axis differs depending on the species group. The light grey kogiid detections at WIL indicate narrow-band high-frequency (NBHF) clicks that occured within the geographic range of harbour porpoises.

2016; Virgili et al., 2019), including those capturing seasonal and sub-seasonal (weekly-to-daily) variability. While topographic variables (e.g. bathymetry depth and slope) are known to be important drivers of deep-diving cetacean foraging behaviour, we did not include depth as we only had seven unique measurements that did not change over time. As such, we recognize that differences between the sites likely reflect the depth of the lander as well as its geographic location and oceanographic context. Satellite and model-derived variables were obtained from daily or 8-day products and at a 1 to ~ 22 km resolution (see Table 3). Daily sea surface temperature was a blended product from multiple satellites and was downloaded via the Copernicus Climate Data Store. Photosynthetically-active radiation represents the cumulative energy in the visible spectrum impinging on the Earth's surface, and chlorophyll-*a* concentration is an indicator of primary productivity. Both products were obtained from NASA's online data archive system. Spatially gridded fields of mixed layer depth were derived from the Hybrid Coordinate Ocean Model (HYCOM) using a 0.125 density contrast. These products were obtained from the Ocean Productivity site maintained by Oregon State University (Table 3). To characterize fronts associated with the Gulf Stream, fine-scale, daily satellite-derived front maps using an established composite front-mapping method were acquired (Miller, 2009; Miller et al., 2015). Single-Image Edge Detection (Cayula and Cornillon, 1992) was applied to SST layers using a detection threshold of 0.4 °C (Miller, 2009) and the following raster grids were created: 1) distance to closest front (km), 2) front gradient density (scalar value of 0–1), a measure of the strength of frontal gradients, and 3) front persistence (0–1), the proportion of cloud-free observations of a pixel that a front is detected, averaged over a 7-day sliding window. Additionally, we considered backward-in-time finite-size Lyapunov exponent which measures the dispersion of particles over current velocity fields and is an indicator of convergence and divergence of waters masses, which was a delayed-time product downloaded directly from AVISO.

To characterize currents and eddies, daily sea level anomaly and absolute dynamic topography satellite altimeter data were obtained from AVISO via Copernicus Marine Service (CMEMs). We considered three variables: 1) sea level anomaly (m) as an indication of cyclonic (negative anomaly) and anticyclonic (positive anomaly) eddies, 2) eddy kinetic energy (m/s) defined as the energy associated with the turbulent part of the flow, which was calculated based zonal and meridional geostrophic velocity anomalies, and 3) total kinetic energy as an indicator of the strength of the Gulf Stream, calculated from geostrophic velocities (see Appendix A for details). A buffer with a 10 km radius was created around each lander location using the *rgeos* package *v.* 0.5–9 (Bivand et al., 2020) and the mean value for each variable was calculated using the *raster* package *v.* 3.6.14 (Hijmans et al., 2021). We note that this buffer size is larger than the acoustic propagation range for the study species, particularly kogiids (450 m; Malinka et al. 2021), however this value roughly corresponded to the average spatial resolution of the environmental variables that we considered (Table 3). Lastly, the *lunar* package *v.* 0.1.4 (Lazaridis, 2014) was used to calculate a daily value of lunar illumination associated with each site.

2.4. Statistical analyses

Generalized additive (mixed) models (GAM[M]s) in the *mgcv* package *v.* 1.8.38 (Wood, 2017) were used to model the potential non-linear relationships between covariates and detection positive hours for each cetacean species or group. Delphinids were not considered, as this group encompasses species with a wide range of habitat and prey preferences. We considered two sets of models: one "global" model including data from all sites where that group was automatically detected (excluding locations where species were never manually confirmed or were confirmed but the automated detector performance was low), and separate site-specific models to quantify species-environment relationships at specific sites. Global GAMMs were only run for kogiids, which were detected at three lander sites, with site identity included as a random effect. Due to the low detection probability of kogiids at sites other than BLE, only one site-specific model was run for kogiids, while models were also run for Blainville's beaked whales at BLE and Gervais'/True's beaked whales at SAV. Detection positive hours were modelled using a negative binomial distribution due to the skewed distribution and high number of zero observations in many datasets.

We followed an information-theoretic model comparison approach to test multiple hypotheses. For the global and site-specific models, we ran a series of candidate models consisting of variables representing near-surface oceanographic processes or features that we hypothesize to influence foraging behaviour, as well as the lunar cycle (see Table 2 for details), and compared these models to both the null model and a full model containing all environmental covariates. To prevent over-parameterization, the number of knots was limited to five and splines were produced using cubic regression with shrinkage, allowing covariates to be penalized out of the model entirely during fitting. Before running candidate sets, multicollinearity between variables was tested using Spearman rank correlations and variance inflation factors (VIF), and correlated variables (>0.6 correlation coefficient, VIF > 3) were removed from analyses. Front gradient density and persistence were highly correlated, so we only included the latter, while in all cases, mixed layer depth was correlated with sea surface temperature and chlorophyll-*a* concentration and so was not considered. Also, for the Blainville's model, total and eddy kinetic energy were correlated, and given models with the former resulted in a lower Akaike Information Criterion (AIC) score, total kinetic energy was used. Several variables were transformed before inputting into models to improve data spread (see Appendix A). Cloud cover prevented satellite coverage for chlorophyll-*a* data, so we removed days with NA values (13 % of total). A comparison of missing values across the year revealed no clear seasonal

Table 2
Candidate models representing oceanographic processes and their proposed importance to foraging deep-diving odontocetes.

	Model name	Justification	Covariates
1	Null	Potential site and year differences in detections but no effect of oceanography.	Year
2	Sea surface temperature	Detections relate to seasonal and regional variation in sea surface temperature and associated thermal tolerance and prey community preferences.	SST, Year
3	Primary productivity	Detections relate to primary productivity and inferred prey abundance.	Chl, PAR, Year
4	Fronts	Detections relate to the position and persistence/strength of mesoscale fronts, where prey may be concentrated and retained, or subducted to form denser deep-scattering layers.	FDist, FPers, Year
5	Mesoscale activity	Detections relate to the intensity of currents, meanders and eddy activity associated with the Gulf Stream. Eddies, currents and meanders transport prey horizontally and may interact with bathymetry to aggregate prey. Eddies may also downwell and concentrate micronekton in the mesopelagic, attracting fish and squid.	TKE, EKE, FSLE, SLA, Year
6	Mixed layer	Detections relate to depth of the mixed layer. A shallow mixed layer may concentrate biomass and attract nekton from deeper waters. A deeper mixed layer may push the thermocline deeper and spread the deep-scattering layer vertically into the preferred depths of deep-diving cetaceans.	MLD, Year
7	Lunar	Detections relate to inferred strength of prey diel vertical migration.	Lunar, Year

See Table 3 for full names of covariates.

Table 3
Sources and resolution of oceanographic variables considered.

Abbrev.	Variable	Units	Source	Satellite (S) or model (M)	Resolution Spatial	Temporal
SST	Sea surface temperature	°C	Copernicus Climate Data Store[1]	Multiple satellites (S)	0.05° (~4–5 km^2)	Daily
Chl	Chlorophyll-*a* concentration	mg/m3	NASA Goddard via Ocean Color[2]	VIIRS (S)	4.6 km^2	8-day mean
PAR	Photosynthetically-active radiation	$mol/m^2/d$				
FDist	Front distance	km	NASA JPL	GHRSST MUR (S)	1 km^2	Daily
FPers	Front persistence*	Scalar value: 0–1				Daily, avg. over 7-day window
FSLE	Finite-size Lyapunov exponent	d^{-1}	AVISO[3]	SSALTO/DUACS (S)	1/25° (4 km^2)	Daily
EKE	Eddy kinetic energy	m/s	AVISO via CMEMs[4]	SSALTO/DUACS (S)	0.25° (~22–23 km^2)	Daily
TKE	Total kinetic energy	m/s				
SLA	Sea level anomaly	m				
MLD	Mixed layer depth	m	Oregon State University[5]	HYCOM (M)	12.5 km^2	8-day mean

[1]https://doi.org/10.24381/cds.cf608234; [2]https://oceancolor.gsfc.nasa.gov; [3]https://www.aviso.altimetry.fr/en/data/products/value-added-products/fsle-finite-size-lyapunov-exponents.html, [4]https://doi.org/10.48670/moi-00148; [5]https://www.hycom.org/.
NASA = National Aeronautics and Space Administration; VIIRS = Visible Infrared Imaging Radiometer Suite; GHRSST = Group for High Resolution Sea Surface Temperature; MUR = Multiscale Ultrahigh Resolution; JPL = Jet Propulsion Laboratory; AVISO = Archiving, Validation and Interpretation of Satellite Oceanographic data; SSALTO/DUACS = Segment Sol Multimission Altimetry and Orbitography/Data Unification and Altimeter Combination System; CMEMS = Copernicus Marine Service; HYCOM = Hybrid Coordinate Ocean Model.
*Front gradient density (FGrad) was always highly correlated with front persistence density so was not considered for formal analyses.

pattern that was consistent across sites (Fig. A1 in Appendix A).

Candidate models were ranked according to AIC with the best model considered to be that with the lowest score. In cases where there were several models within two AIC units of the best supported model, the most parsimonious model, i.e. that with the fewest parameters, was chosen. We also calculated the deviance explained by each model and used *k*-folds cross-validation with relative root mean square error (RRMSE) to assess model performance. Iteratively ten times, 70 % of the data were used to train the model, which was tested on the remaining 30 %. RRMSE was calculated by dividing the root mean square error, the average difference between predicted and observed values, by the range of the response variable and expressing as a percentage, making it easier to compare across different species groups. Serial autocorrelation in model residuals was examined using autocorrelation function (ACF) plots and temporal autocorrelation tests in the *DHARMa* package *v.* 0.4.6 (Hartig, 2022). The inclusion of year as a covariate in all models substantially reduced autocorrelation (Fig. A2 in Appendix A), though, there was still some residual autocorrelation for the Blainville's beaked whale and kogiid (both for BLE and all sites) models, which could not be reduced by further inclusion of an autocorrelation term. Overdispersion statistics, QQ and residual plots in the *mgcViz* package *v.* 0.1.9 (Fasiolo et al., 2021) were used to assess model fit (Zuur et al., 2009).

Lastly, we tested for diel variation using hourly presence/absence data, which were categorized according to photoperiod (daylight, twilight or darkness) using the crepuscule function in the *maptools* package *v.* 1.1.2 (Bivand and Lewin-Koh, 2021). Twilight periods were defined as the time between civil dawn (when the sun is 6° below the horizon) and sunrise, and between sunset and civil dusk. A series of binomial GAMs were run for each species to test whether time of day (hours since midnight) or photoperiod influenced the probability of detection. We built the models for each species group with the following covariates: 1) null model (no covariates), 2) year, 3) year and a smooth spline for time of day, 4) year and a cyclical spline for time of day, and 5) year and photoperiod. For kogiids we also included site as a fixed effect and ran a further set of models containing the interaction of site with the 6) smoothed and 7) cyclical effect of time of day and 8) photoperiod, to test for site-specific patterns. We ran models with the number of knots for continuous variables increased up to eight and selected the value which yielded models with the lowest AIC. To reduce temporal autocorrelation, we ran models using the bam function in the *mgcv* package, which better handles large datasets and allows for the inclusion of a first-order autoregressive (AR1) term. The AR1 correlation parameter was chosen for each species using the *itsadug* package *v.* 2.4.1 package (van Rij et al., 2022). We used ACF plots to determine the most appropriate size of grouping blocks, within which data are known to be correlated, and included this blocking factor in models. Autocorrelation tests (as above) confirmed that residuals were not temporally autocorrelated. For each species, the most parsimonious models were selected through model comparison using AIC. Unless otherwise specified, means are provided ± standard deviations.

3. Results

3.1. Regional and seasonal variation in detections

Passive acoustic monitoring was carried out at seven sites over a three-year period (2017–2020), yielding a total of 7491 days of data across all sites (Table 1). Odontocetes (including delphinids) were recorded at all sites (Fig. 2). Broad patterns of occurrence based on automated detections generally followed those of manual detections (presented in Kowarski et al., 2023). However, there were manual detections of species not reliably identified by the automated detector-classifier which were not included in further analyses: kogiids at JAX, Blainville's beaked whales at SAV, goose-beaked whales at BLE, and Gervais'/True's beaked whales at VAC and WIL.

There was substantial daily variation in cetacean positive hours based on automated detectors, as well as variation between species groups and sites (Fig. 2). Kogiids were detected at BLE (75.2 % of days), SAV (12.4 %) and CHB (3.3 %) (Fig. 2b). At BLE, kogiids were consistently recorded throughout the study period, up to 7 h/day (mean = 2.2 ± 1.3 when present), with no clear evidence of seasonality in detection rates. In contrast, most days when kogiids were detected at SAV (72.9 %) and CHB (88.9 %) occurred during winter and spring (December–May). Gervais'/True's beaked whales were detected only at SAV, present on 12.9 % of days for up to 5 h/day (mean = 1.4 ± 0.8), and with higher occurrence in 2019 (17.0 % of days) and 2020 (18.0 %) than 2017 (5.9 %) and 2018 (4.5 %) (Fig. 2c). Blainville's beaked whales were only detected at BLE and consistently throughout the study period but were recorded less often than kogiids (28.0 % of days), up to 6 h/day (mean = 1.4 ± 0.7) (Fig. 2d).

3.2. Oceanographic and lunar influences on cetacean detections

The best models explaining kogiid detections across multiple lander

sites (global models) were the full models containing all covariates (Table 4), performing well with a high deviance score of 59.7 %. However, much of the explanatory performance was explained by the random effect of site, with the deviance varying by ~ 1 % between the best and worst performing model sets. Models representing primary productivity, mesoscale activity and sea surface temperatures all performed substantially better than the null model according to AIC. Detection positive hours increased with chlorophyll-*a* concentrations above ~ 0.15 mg/m^3, generally indicative of mesotrophic waters, and was marginally higher with lower current speeds (total kinetic energy < 0.6 m/s), and increased eddy kinetic energy, but there was no clear pattern to the effect of sea surface temperature (Fig. 3a–c).

Site-specific models revealed that the mesoscale activity model was the best for kogiids at BLE, yet it explained a negligible amount of deviance (<4%; Table 4) with only marginal effects of covariates, including a slight increase in detection positive hours with current speeds around 0.05–0.20 m/s (Fig. 3d), though this is well below the average speed of the Gulf Stream (1–2 m/s, Fig. 1e and f, Fig. 4d). Model predictions were not able to track weekly to monthly variation in detection positive hours (Fig. 5a), suggesting other unmodelled processes are likely to be important. For Blainville's beaked whales at BLE, the best model included all covariates, with the mesoscale activity model performing slightly better than the lunar model, yet all had low explanatory power (<7 % deviance explained; Table 4). Blainville's beaked whale detections were strongly influenced by lunar illumination (Fig. 3e) and elevated activity appeared to coincide with the full moon, though not in every instance (Fig. 5b). Detection positive hours were also marginally higher in moderate sea level anomaly (0.1–0.3 m) and high sea surface temperatures (>26 °C, Fig. 3f and g). The best-performing Gervais'/True's BLE model was also that with all covariates and performed moderately well (21 % deviance explained). Detections were higher on days with low photosynthetically-active radiation, higher eddy kinetic energy and negative sea level anomaly, indicative of cyclonic eddies (Fig. 3h–j). Peaks in detections were often associated with elevated eddy activity (Fig. 4e, Fig. 5c). For all species, there did not appear to be an effect of frontal metrics (Table 4).

3.3. Diel variation in detections

The best models explaining diel variation in detection probability differed according to species group (Fig. 6, Table A3). For kogiids, the best model contained the smoothed effect of time of day, and the detection probability at the two deepest sites was consistently higher during the period from dawn to an hour after sunrise and from a few hours before sunset to sunset (Fig. 6a and b). There was no clear diel pattern for kogiids at CHB. While there was no significant effect of time of day or photoperiod for Blainville's beaked whales, for Gervais'/True's beaked whales the probability of detection was marginally higher during darkness than daylight (parameter estimate ± standard error: 0.40 ± 0.15; Fig. 6c and d) and varied in a non-linear way according to time of day for kogiids.

Table 4
Single- and multi-site generalized additive (mixed) models (GAM[M]s) examining the effects of oceanography and lunar illumination on detection positive hours (DPH) of kogiids, Gervais'/True's beaked whales and Blainville's beaked whales. The best supported model in each case is shown in bold and the null model in italics.

Model	Covariates	AIC	ΔAIC	Dev.	RRMSE (%)
Kogiid whales: multi-site (CHB, SAV, BLE)					
Full	**Chl, TKE, EKE, FPers, TKE, FDist, SLA, FSLE, PAR, Lunar, Year**	**3901.3**	**0.0**	**59.7**	6.1
Productivity	Chl, PAR, Year	3908.0	6.7	59.4	**5.9**
Mesoscale activity	TKE, SLA, EKE, Year	3923.8	22.5	59.0	6.4
Mixed layer	MLD, Year	3923.8	22.5	58.9	6.2
Sea surface temperature	SST, Year	3925.6	24.3	58.8	6.2
Fronts	FPers, FDist, FSLE, Year	3930.2	28.8	58.7	6.2
Null	*Year*	3930.6	29.3	58.6	6.3
Lunar	Lunar, Year	3930.6	29.3	58.6	6.3
Kogiid whales: single-site (BLE)					
Full	TKE, Chl, FPers, EKE, PAR, SLA, FDist, Lunar, FSLE, SST, Year	3036.5	0.0	3.1	5.2
Mesoscale activity	**TKE, EKE, SLA, Year**	**3037.4**	**0.9**	**2.7**	5.1
Mixed layer	MLD, Year	3038.1	1.6	2.6	5.1
Productivity	Chl, PAR, Year	3038.9	2.5	2.5	5.1
Fronts	FPers, FDist, FSLE, Year	3039.5	3.0	2.4	5.0
Null	*Year*	*3039.9*	*3.4*	*2.2*	**5.0**
Lunar	Lunar, Year	3039.9	3.4	2.2	5.0
Sea surface temperature	SST, Year	3039.9	3.5	2.2	5.0
Gervais'/True's beaked whales: single-site (SAV)					
Full	**PAR, SLA, EKE, FDist, SST, Chl, FPers, Lunar, FSLE, TKE, Year**	**804.8**	**0.0**	**21.0**	14.2
Productivity	PAR, Chl, Year	813.0	8.2	17.9	13.3
Mesoscale activity	SLA, EKE, TKE, Year	830.7	25.9	13.4	14.1
Mixed layer	MLD, Year	831.2	26.4	12.7	12.8
Sea surface temperature	SST, Year	833.9	29.1	11.8	0.6
Lunar	Lunar, Year	845.6	40.8	9.3	12.5
Null	*Year*	846.3	41.5	8.2	**<0.1**
Fronts	FDist, FPers, FSLE, Year	846.7	41.9	8.8	11.8
Blainville's beaked whales: single-site (BLE)					
Full	**Lunar, SLA, SST, PAR, FSLE, FDist, Chl, TKE, FPers**	**1442.0**	**0.0**	**7.0**	**9.8**
Mesoscale activity*	SLA, TKE, Year	1451.7	9.6	4.6	10.5
Lunar	Lunar, Year	1452.5	10.5	4.4	9.8
Sea surface temperature	SST, Year	1452.6	10.5	4.1	20.1
Productivity	Chl, PAR, Year	1456.3	14.3	4.1	10.7
Mixed layer	MLD, Year	1456.3	14.3	3.8	10.8
Fronts	FDist, FPers, FSLE, Year	1461.1	18.9	2.8	11.0
Null	*Year*	*1461.1*	*19.0*	*2.6*	*48.6*

*TKE and EKE were highly correlated and so only TKE was included. AIC = Akaike information criterion; ΔAIC = change in AIC from the best-supported model; Dev. = % deviance explained; RRMSE = relative root mean square error. The site included in the model is shown for each species: HAT = Hatteras South; CHB = Charleston Bump; SAV = Savannah Deep, JAX = Jacksonville, BLE = Blake Escarpment.

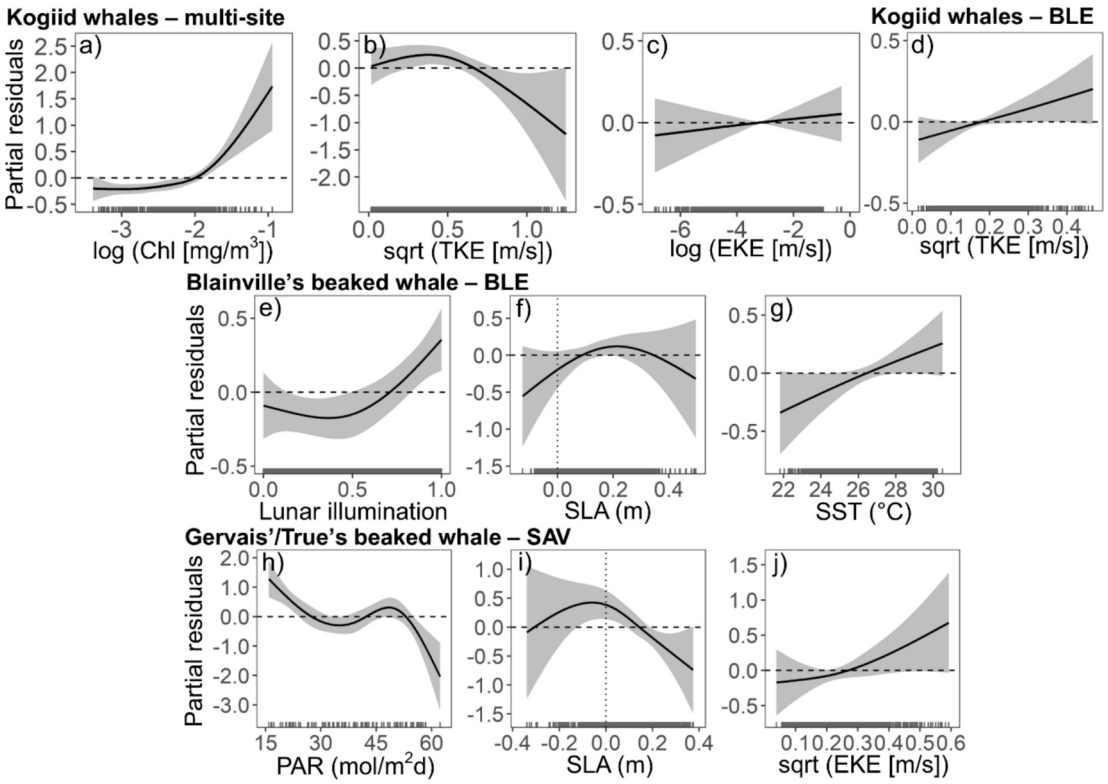

Fig. 3. Responses of deep-diving odontocetes to environmental covariates. Partial plots are shown based on a-c) multi-site generalized additive mixed models (GAMMs) for kogiid whales and d-j) site-specific generalized additive models (GAM) for d) kogiid and e-g) Blainville's beaked whales at Blake Escarpment (BLE), and h-j) Gervais'/True's beaked whales at Savannah Deep (SAV). Predicted 95% confidence intervals shown in grey.

4. Discussion

Using a passive acoustic monitoring dataset spanning three years at seven sites along the northwest Atlantic Outer Continental Shelf, we provide insights into the year-round distributions and influence of near-surface oceanographic features and diel and lunar cycles on foraging vocalizations for a deep-diving cetacean community. We show that foraging activity was associated with several oceanographic indices, including seasonal variation in sea surface temperatures and mesoscale activity at sites near the Gulf Stream; though, the results were site- and species-specific and the proximity and strength of fronts did not have an effect. The influence of lunar and diel cycles on foraging activity also varied by species, likely reflecting species-specific foraging behaviour and site differences in the vertical distribution of prey communities. Overall, findings suggest that habitat use by deep-diving cetaceans is weakly associated with near-surface oceanography, with large unexplained variability that is probably related to prey characteristics and environmental processes occurring at depth.

4.1. Regional and seasonal variation in detections

Kogiid and beaked whales were frequently detected at the deepest sites and the amount of time they spent at a site per day appeared to reflect processes over both relatively short- (i.e. daily to monthly) and longer-term (i.e. seasonal to annual) timescales. These results, based on a much larger dataset of automated detections, strengthen findings based on manual detections (Kowarski et al., 2023) and from other acoustic arrays (e.g. Cohen et al., 2023; DeAngelis et al. 2025), that the Blake Plateau, offshore from Georgia and Florida, is an important foraging habitat for deep-diving cetaceans, with year-round presence of kogiid and beaked whales. Through modelling automated detection positive hours, we were able to investigate the extent to which foraging odontocetes were present at or near sites throughout the day. However, we note that the results are influenced by automated detector-classifier performance, which was variable for some species and sites. We were also unable to reliably capture the vocalizations of sperm whales, which were present at all sites, or goose-beaked whales, which were detected on three occasions at BLE (Kowarski et al., 2023), and for which there is a resident population in deeper waters off the Mid-Atlantic Bight (Foley et al., 2021; Shearer et al., 2019).

Kogiids were detected at BLE for up to 7 h/day, but without clear seasonality, suggesting year-round residency. This lack of seasonality mirrors stranding records in the southeastern U.S. (Hodge et al., 2018) and detections around Hawai'i (Ziegenhorn et al., 2023), where photo-identification also indicates kogiids have small home ranges (Baird et al., 2022). The finding that the two beaked whale groups (Blainville's and Gervais'/True's) are continuously present at separate latitudes supports previous studies demonstrating segregation of beaked whales along the Atlantic seaboard (Cohen et al., 2023; Kowarski et al., 2023; Stanistreet et al., 2017). Similar to kogiids, beaked whales are likely to exhibit year-round presence, as observed in this region and elsewhere (e.g. Cohen et al., 2023; Henderson et al., 2016; Stanistreet et al., 2017). While True's or Gervais' beaked whales could not be classified at the species level, given that previous studies have not detected True's beaked whales south of the Norfolk Canyon (near the VAC lander site), it is likely that this acoustic group at SAV represents Gervais' beaked whales (DeAngelis et al., 2025; Kowarski et al., 2023; Stanistreet et al., 2017).

4.2. Oceanographic drivers of detections

Variables reflecting both seasonal and mesoscale changes in the environment were often the most important drivers of vocal detections. Previous studies have demonstrated the importance of topographic features for deep-diving whale distributions and foraging activity (e.g. Roberts et al., 2016), though due to our study design and the limited

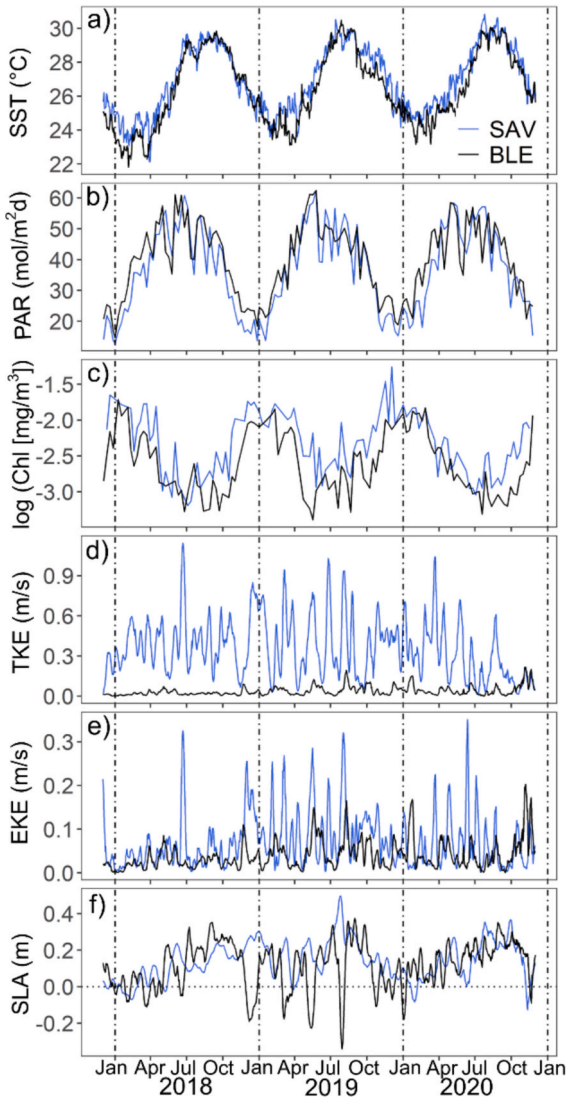

Fig. 4. Time series of near-surface oceanographic variables considered important to deep-diving odontocetes at the two deepest lander sites, Savannah Deep (SAV; blue) and Blake Escarpment (BLE; black) from 2017 to 2020. SST: sea surface temperature, PAR: photosynthetically-active radiation, Chl: chlorophyll-*a* concentration, TKE: total kinetic energy, EKE: eddy kinetic energy, SLA: sea level anomaly. The vertical dashed lines indicate the start of each calendar year.

number of sites and associated depth values, we were not able to include temporally static covariates. In multi-site models, the effect of site was by far the strongest driver of variability, and could represent differences between sites in depth and topography, latitudinal differences in habitat suitability, as well as other unmodelled processes. It is clear though that the depth of sites is likely an important factor explaining the acoustic presence and time spent by deep-diving species, as beaked whales were only detected at the two deepest sites (≥790 m) and kogiids were detected much more frequently and for longer at the deepest site (BLE). The lack of beaked whale detections at northern sites is also likely a function of the shallow depth of landers (<300 m) rather than true absences in the region.

At the seasonal scale, Blainville's beaked whale activity was slightly higher in late summer when sea surface temperatures were higher. This preference for warmer temperatures (>26 °C) supports other studies in the region that showing they are the most tropical and southerly distributed beaked whale species in the South Atlantic Bight, preferring waters > 28–29 °C (e.g., Cohen et al. 2023; DeAngelis et al., 2025). In contrast, there was no apparent seasonality in detections for kogiids. As we predicted, several variables were important at the mesoscale and sub-mesoscale, however their effects were generally modest. Both kogiid and Gervais'/True's beaked whales had higher foraging activity with increased eddy kinetic energy, which supports findings from at-sea surveys in the Mid-Atlantic Bight, which have found greater densities of kogiid and (unidentified) beaked whales in regions with higher eddy kinetic energy (Roberts et al. 2016, Virgili et al. 2019) and acoustic studies which have found higher detections of Gervais' beaked whales in highly dynamic but lower productivity Gulf Stream waters (DeAngelis et al. 2025). In the South Atlantic Bight, eddies are often generated around the Charleston Bump and either propagate westward towards the coast or north-eastward along the Gulf Stream, where their amplitude increases with water depth (Castelao and He, 2013). For Gervais'/True's beaked whales, which were detected just east of the Charleston Bump (at SAV), increased foraging activity was also associated with negative sea level anomaly, indicative of cyclonic eddies which may serve to transport cooler shelf or slope waters offshore (Lee et al., 1991). Cyclonic eddies can enhance local productivity by upwelling nutrients from below the mixed layer into the photic zone, typically increasing surface chlorophyll-*a* concentrations (Gaube et al., 2014). Sperm whale sightings are elevated around these features (Frasier et al., 2021), suggesting that the enhanced surface productivity has an aggregative influence on zooplankton and nekton prey in waters far below the mixed layer. Cyclonic eddies may also increase prey accessibility to deep-diving cetaceans by shoaling the deep-scattering through the upward bending of isotherms (Wang et al., 2024). However, because Gervais' beaked whales dive deeper than this (around 870 m on average; DeAngelis et al. 2025), the exact mechanisms through which mesoscale activity influences foraging via the distribution and aggregation patterns of their predominantly cephalopod and crustacean prey (MacLeod et al. 2003, Santos et al. 2007), remain unclear.

While various deep-diving species are known to target regions of elevated frontal activity in the northwest Atlantic Ocean (Virgili et al., 2019; Waring et al., 2001), we found that at sub-mesoscales, there was no significant relationship between foraging activity and metrics of frontal persistence or distance, nor finite-size Lyapunov exponent, which is a dynamic indicator of areas of water mass convergence and divergence. This could be partly related to our study design; those sites associated with the greatest frontal activity were at shallower sites, and at deeper sites where deep-diving species were detected, frontal activity was relatively low. Also, it could be that the effect of fronts on prey biomass at depth is lagged and requires persistent frontal activity for aggregative effects on predator behaviour to become pronounced (e.g. Miller et al., 2015; Scales et al., 2014b), or that surface manifestations are spatially offset from their effects on prey at depths where deep-divers forage. We recommend future studies that can monitor deeper sites in regions of high frontal activity, such as around the Hatteras Front, perhaps in combination with biologging and active acoustics, to examine their influence on the fine-scale foraging behaviour of deep-diving whales.

4.3. Diel variation and relationships with the lunar cycle

Mesopelagic prey communities often migrate vertically within the water column as a function of light levels to maximize foraging success, while simultaneously minimizing predation risk, on both a daily basis and as a function of lunar phase (Benoit-Bird et al., 2009; Urmy and Benoit-Bird, 2021). One of the more striking patterns we found was the cyclical nature of Blainville's beaked whale detections at BLE that tracked the lunar cycle, with elevated foraging activity during the full moon. While relatively few studies have investigated lunar influences on beaked whale foraging, acoustic and tagging studies in Hawai'i have shown that Blainville's beaked whales forage more and deeper during periods of high lunar illumination (Baird, 2019; Henderson et al., 2016). The increase in detection positive hours of Blainville's beaked whales in

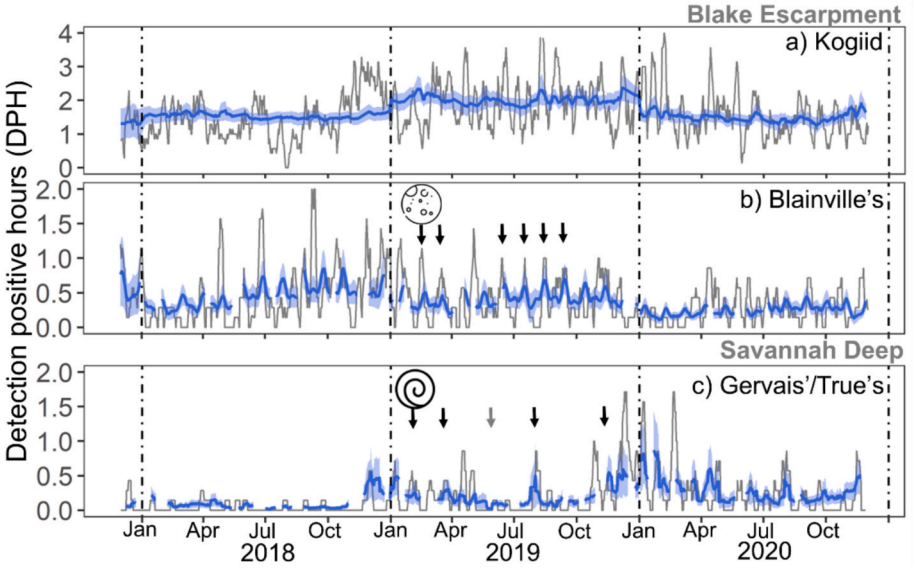

Fig. 5. Time series of observed and predicted detection positive hours (DPH) for a) kogiid, and b) Blainville's beaked whales at Blake Escarpment (BLE) and c) Gervais'/True's beaked whales at Savannah Deep (SAV) from 2017 to 2020. For plotting purposes, observed DPH was smoothed over a 7-day moving window and is shown by grey lines. The predicted time series from site-specific generalized additive models (GAMs) are shown by blue lines with 95% confidence intervals in blue shading. The vertical dashed lines indicate the start of each calendar year. b) Blainville's beaked whale DPH is elevated during the full moon (black arrows), while c) Gervais'/True's beaked whale DPH is elevated during periods of high eddy kinetic energy (black arrows); though, one example when vocal activity is not elevated is shown (grey arrow).

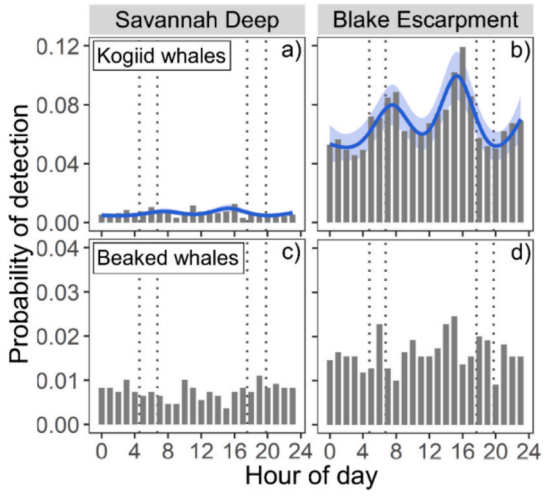

Fig. 6. Diel variation in the probability of detection of a-b) kogiid and c-d) beaked whales, at the two deep lander sites, Savannah Deep (SAV; left column) and Blake Escarpment (BLE; right column). The mean probability of detection for each species group, site and hour is shown by grey bars and the smoothed relationship based on generalized additive (mixed) models (GAM[M]s) is shown by a blue line, with confidence intervals in lighter shaded blue. Hour of day did not have a significant effect of beaked whale probability of detections and the relationship is not shown. The dashed vertical lines represent the minimum and maximum timing of dawn and dusk across the year for the two sites.

this study could reflect either process, as well as the horizontal movement of individuals along the continental slope. Regardless, during the full moon prey in the scattering layer are expected to remain deeper and more concentrated in the water column (Prihartato et al., 2016), making them potentially easier targets for foraging beaked whales within the deeper waters of the Blake Plateau.

Diel patterns of detections differed among the species groups, and as predicted there were stronger effects for kogiids than beaked whales, generally supporting past findings. For kogiids, there were two echolocation peaks, in the hours after sunrise and before sunset, respectively. Studies in Hawai'i and the Gulf of Mexico have shown kogiid detections to be higher during the day at some sites (Hildebrand et al. 2019, Ziegenhorn et al. 2023). As with the effect of the lunar cycle, it is unclear whether these patterns relate to changes in foraging activity, or the distribution or orientation of echolocating animals. However, given that kogiids feed on a diversity of micronekton in the meso- and bathypelagic at depths between 400 and 1000 m (Beatson, 2007; West et al., 2009) it is likely they are foraging deeper during daylight hours (Hildebrand et al., 2019) and thus echolocating nearer or in the direction of the bottom-mounted hydrophone. In contrast, we found no diel pattern for beaked whales, which mirrors other studies in the region (Cohen et al., 2023; Shearer et al., 2019). Blainville's beaked whales consistently do not appear to change their foraging depth distribution between day and night, probably because they feed in depths of perennial darkness and target lower levels of the deep scattering later that may not migrate, or squid and deepwater fish below at depths of between 800 and 1400 m (Arranz et al., 2011; Baird et al., 2006; Hazen et al., 2011). Indeed, a recent study based on acoustic towed arrays in the region showed dive depths of Blainville's beaked whales to be 960 m on average, with all dives in waters shallower than 3000 m occurring in proximity to the seafloor (DeAngelis et al., 2025); this suggests that animals at BLE are probably feeding on prey near or on the seafloor.

5. Conclusions

Our study confirms that the U.S. Outer Continental Shelf, and particularly the deeper waters associated with the Blake Plateau, are important year-round foraging habitats for kogiid and beaked whales. This region is generally poorly monitored and not well represented in at-sea surveys (e.g. Roberts et al., 2016; Virgili et al., 2019) or by passive acoustic monitoring (e.g. Cohen et al., 2023; Stanistreet et al., 2017), but likely supports significant numbers of cetaceans, given its large extent and suitable depth (500–1000 m). Deep-diving odontocetes are sensitive to noise pollution from sources such as military sonar, ship noise and explosive sounds, which are all present within the study region (Rafter et al., 2021). The apparent patterns of residency identified here indicate that repeated exposure may not only have acute but chronic impacts

(Simonis et al., 2020; Tyack et al. 2011). As such, extractive activities such as the expansion of mesopelagic fisheries, offshore drilling and deep-sea mining, as well as the development of new offshore wind platforms, should identify critical habitats and the effects of such anthropogenic activities on the physiology and population dynamics of these sensitive and poorly-studied species.

Here, we found associations with near-surface oceanographic variables representing both seasonal trends and mesoscale features, such as eddies, and the foraging activity of Gervais'/True's beaked whales, while lunar phase was also important for Blainville's beaked whales. While we found no oceanographic variables sufficiently explained variation in kogiid detections, our results suggest they are year-round residents that are responsive to the vertical distribution of their mesopelagic prey. Given the complex relationships of some species with oceanographic variables and relatively poor explanatory power of models, it is likely that unmodelled oceanographic processes and prey characteristics at depth, are important determinants of foraging activity. We highlight the need for studies across a greater range of sites that can also integrate sub-surface oceanography with measures of vertical prey distribution, to examine the specific roles of mesoscale features in aggregating prey for predators at depth (Hazen et al., 2011; Virgili et al., 2021).

CRediT authorship contribution statement

Thomas A. Clay: Conceptualization, Methodology, Software, Validation, Formal analysis, Visualization, Writing – original draft. **Gemma Carroll:** Writing – review & editing, Methodology, Conceptualization. **Megan A. Cimino:** Writing – review & editing, Methodology, Conceptualization. **Jennifer L. Miksis-Olds:** Writing – review & editing, Project administration, Investigation, Funding acquisition, Conceptualization. **Katie Kowarski:** Writing – review & editing, Validation, Methodology, Formal analysis, Data curation. **Anthony P. Lyons:** Project administration, Investigation, Funding acquisition, Conceptualization. **Peter I. Miller:** Writing – review & editing, Investigation. **Timothy Moore:** Writing – review & editing, Resources, Data curation. **Joseph D. Warren:** Writing – review & editing, Resources, Project administration, Investigation, Funding acquisition, Conceptualization. **Elliott L. Hazen:** Writing – review & editing, Supervision, Methodology, Funding acquisition, Conceptualization.

Declaration of competing interest

The authors declare that they have no known competing financial interests or personal relationships that could have appeared to influence the work reported in this paper.

Acknowledgements

Study concept, oversight and funding for the Atlantic Deepwater Ecosystem Observatory Network (ADEON) were provided by the US Department of the Interior, Bureau of Ocean Energy Management, Environmental Studies Program, Washington, DC, under contract number M16PC00003, in partnership with the Office of Naval Research (ONR) and the National Oceanic and Atmospheric Administration (NOAA). Funding for ship time was provided under separate contracts by ONR, Code 32. We are grateful to the ship and crews of the RV 'Neil Armstrong', RV 'Endeavor' and ROV JASON for their support during data collection, Bruce Martin for designing the bottom-lander network and supporting acoustic data analyses, John Macri for managing the project and Theresa Ridgeway for support with data management. We thank Andy Read for useful discussions and Adena Schonfeld, the Associate Editor Meng Xia and two anonymous reviewers for insightful feedback on earlier versions of this manuscript.

Appendix A. Supplementary data

Supplementary data to this article can be found online at https://doi.org/10.1016/j.pocean.2025.103581.

Data availability

The raw acoustic recordings from ADEON are available through the National Center for Environmental Information (NCEI; https://ncei.noaa.gov). Hourly mammal acoustic presence data and visual marine mammal sightings data are available from the ADEON website (see https://adeon.unh.edu/).

References

Abrahms, B., Scales, K.L., Hazen, E.L., Bograd, S.J., Schick, R.S., et al., 2018. Mesoscale activity facilitates energy gain in a top predator. Proc. R. Soc. B 285, 20181101.
Acha, E.M., Piola, A., Iribarne, O., Mianzan, H., 2015. Ecological Processes at Marine Fronts: oases in the ocean, Springer Briefs in Environmental Science. Springer International Publishing.
Arostegui, M.C., Gaube, P., Woodworth-Jefcoats, P.A., Kobayashi, D.R., Braun, C.D., 2022. Anticyclonic eddies aggregate pelagic predators in a subtropical gyre. Nature 609, 535–540.
Arranz, P., de Soto, N.A., Madsen, P.T., Brito, A., Bordes, F., Johnson, M.P., 2011. Following a Foraging Fish-Finder: Diel Habitat use of Blainville's Beaked Whales Revealed by Echolocation. PLoS One 6, e28353.
Bailleul, F., Cott, C., Guinet, C., 2010. Mesoscale eddies as foraging area of a deep-diving predator, the southern elephant seal. Mar. Ecol. Prog. Ser. 408, 251–264.
Baird, R.W., Webster, D.L., McSweeney, D.J., Ligon, A.D., Schorr, G.S., Barlow, J., 2006. Diving behaviour of Cuvier's (Ziphius cavirostris) and Blainville's (Mesoplodon densirostris) beaked whales in Hawai'i. Can. J. Zool. 84, 1120–1128.
Baird, R.W., 2019. Behavior and Ecology of Not-So-Social Odontocetes: Cuvier's and Blainville's Beaked Whales. In: Würsig, B. (Ed.), Ethology and Behavioral Ecology of Odontocetes. Springer International Publishing, pp. 305–329.
Baird, R.W., Mahaffy, S.D., Lerma, J.K., 2022. Site fidelity, spatial use, and behavior of dwarf sperm whales in hawaiian waters: using small-boat surveys, photo-identification, and unmanned aerial systems to study a difficult-to-study species. Mar. Mamm. Sci. 38, 326–348.
Barlow, J., Schorr, G.S., Falcone, E.A., Moretti, D., 2020. Variation in dive behavior of Cuvier's beaked whales with seafloor depth, time-of-day, and lunar illumination. Marine Ecology Progress Series 644, 199–214.
Baumann-Pickering, S., McDonald, M.A., Simonis, A.E., Solsona Berga, A., Merkens, K.P. B., et al., 2013. Species-specific beaked whale echolocation signals. J. Acoust. Soc. Am. 134, 2293–2301.
Beatson, E., 2007. The diet of pygmy sperm whales, Kogia breviceps, stranded in New Zealand: implications for conservation. Rev. Fish Biol. Fish. 17, 295–303.
Belkin, I.M., Cornillon, P.C., Sherman, K., 2009. Fronts in Large Marine Ecosystems. Prog. Oceanogr. 81, 223–236.
Benoit-Bird, K.J., Au, W.W.L., Wisdoma, D.W., 2009. Nocturnal light and lunar cycle effects on diel migration of micronekton. Limnol. Oceanogr. 54, 1789–1800.
Benoit-Bird, K.J., Southall, B.L., Moline, M.A., 2019. Dynamic foraging by Risso's dolphins revealed in four dimensions. Mar. Ecol. Prog. Ser. 632, 221–234.
Bivand R, Lewin-Koh N (2021) maptools: Tools for Handling Spatial Objects.
Bivand R, Rundel C, Pebesma E, Stuetz R, Hufthammer KO, et al. (2020) rgeos: Interface to Geometry Engine - Open Source ('GEOS').
Block, B.A., Jonsen, I.D., Jorgensen, S.J., Winship, A.J., Shaffer, S.A., et al., 2011. Tracking apex marine predator movements in a dynamic ocean. Nature 475, 86–90.
Braun, C.D., Arostegui, M.C., Thorrold, S.R., Papastamatiou, Y.P., Gaube, P., et al., 2022. The Functional and Ecological significance of Deep Diving by Large Marine Predators. Ann. Rev. Mar. Sci. 14, 129–159.
Braun, C.D., Della Penna, A., Arostegui, M.C., Afonso, P., Berumen, M.L., et al., 2023. Linking vertical movements of large pelagic predators with distribution patterns of biomass in the open ocean. PNAS 120 (47), e2306357120.
Braun, C.D., Gaube, P., Sinclair-Taylor, T.H., Skomal, G.B., Thorrold, S.R., 2019. Mesoscale eddies release pelagic sharks from thermal constraints to foraging in the ocean twilight zone. PNAS 116 (35), 17187–17192.
Carroll, G., Brodie, S., Whitlock, R., Ganong, J., Bograd, S.J., et al., 2021. Flexible use of a dynamic energy landscape buffers a marine predator against extreme climate variability. Proc. R. Soc. B 288, 20210671.
Castelao, R.M., He, R., 2013. Mesoscale eddies in the South Atlantic Bight. J. Geophys. Res. Oceans 118, 5720–5731.
Cayula, J.-F., Cornillon, P., 1992. Edge Detection Algorithm for SST Images. J Atmos. Ocean. Tech. 9, 67–80.
Chelton, D.B., Gaube, P., Schlax, M.G., Early, J.J., Samelson, R.M., 2011. The Influence of Nonlinear Mesoscale Eddies on Near-Surface Oceanic Chlorophyll. Science 334, 328–332.
Cohen, R.E., Frasier, K.E., Baumann-Pickering, S., Hildebrand, J.A., 2023. Spatial and temporal separation of toothed whales in the western North Atlantic. Mar. Ecol. Prog. Ser. 720, 1–24.
Cohen, R.E., Frasier, K.E., Baumann-Pickering, S., Wiggins, S.M., Rafter, M.A., et al., 2022. Identification of western North Atlantic odontocete echolocation click types using machine learning and spatiotemporal correlates. PLoS One 17, e0264988.

DeAngelis, A.I., Stanistreet, J.E., Baumann-Pickering, S., Cholewiak, D.M., 2018. A description of echolocation clicks recorded in the presence of True's beaked whale (Mesoplodon mirus). J. Acoust. Soc. Am. 144, 2691–2700.
DeAngelis, A.I., Westell, A., Baumann-Pickering, S., Bell, J., Cholewiak, D., et al., 2025. Habitat utilization by beaked whales in the western North Atlantic Ocean using passive acoustics. Mar. Ecol. Prog. Ser. 754, 137–153.
Della Penna, A., Gaube, P., 2020. Mesoscale Eddies Structure Mesopelagic Communities. Front. Mar. Sci. 7, 454.
Fasiolo M, Nedellec R, Goude Y, Capezza C, Wood SN (2021) mgcViz: Visualisations for Generalized Additive Models.
Foley, H.J., Pacifici, K., Baird, R.W., Webster, D.L., Swaim, Z.T., Read, A.J., 2021. Residency and movement patterns of Cuvier's beaked whales Ziphius cavirostris off Cape Hatteras, North Carolina, USA. Mar. Ecol. Prog. Ser. 660, 203–216.
Frasier, K.E., Garrison, L.P., Soldevilla, M.S., Wiggins, S.M., Hildebrand, J.A., 2021. Cetacean distribution models based on visual and passive acoustic data. Sci. Rep. 11, 8240.
Fregosi, S., Harris, D.V., Matsumoto, H., Mellinger, D.K., Barlow, J., Baumann-Pickering, S., Klinck, H., 2020. Detections of Whale Vocalizations by simultaneously Deployed Bottom-Moored and Deep-Water Mobile Autonomous Hydrophones. Front. Mar. Sci. 7.
Gaube, P., McGillicuddy Jr., D.J., Chelton, D.B., Behrenfeld, M.J., Strutton, P.G., 2014. Regional variations in the influence of mesoscale eddies on near-surface chlorophyll. J. Geophys. Res. Oceans 119, 8195–8220.
Hartig F (2022) DHARMa: Residual Diagnostics for Hierarchical (Multi-Level / Mixed) Regression Models.
Hazen, E.L., Johnston, D.W., 2010. Meridional patterns in the deep scattering layers and top predator distribution in the central equatorial Pacific. Fish. Oceano. 19, 427–433.
Hazen, E.L., Nowacek, D.P., Laurent, L.S., Halpin, P.N., Moretti, D.J., 2011. The Relationship among Oceanography, Prey Fields, and Beaked Whale Foraging Habitat in the Tongue of the Ocean. PLoS One 6, e19269.
Henderson, E.E., Martin, S.W., Manzano-Roth, R., Matsuyama, B.M., 2016. Occurrence and Habitat use of Foraging Blainville's Beaked Whales (Mesoplodon densirostris) on a U.S. Navy Range in Hawaii. Aquat. Mamm. 42, 549–562.
Hijmans RJ, van Etten J, Sumner M, Cheng J, Baston D et al. (2021) raster: Geographic Data Analysis and Modeling.
Hildebrand, J.A., Frasier, K.E., Baumann-Pickering, S., Wiggins, S.M., Merkens, K.P., et al., 2019. Assessing Seasonality and Density from Passive Acoustic monitoring of Signals Presumed to be from Pygmy and Dwarf Sperm Whales in the Gulf of Mexico. Front. Mar. Sci. 6, 66.
Hodge, L.E.W., Baumann-Pickering, S., Hildebrand, J.A., Bell, J.T., Cummings, E.W., et al., 2018. Heard but not seen: Occurrence of Kogia spp. along the western North Atlantic shelf break. Mar. Mamm. Sci. 34, 1141–1153.
Hooker, S.K., de Soto, N.A., Baird, R.W., Carroll, E.L., Claridge, D., et al., 2019. Future Directions in Research on Beaked Whales. Front. Mar. Sci. 5, 514.
Johnson, M., Madsen, P.T., Zimmer, W.M.X., de Soto, N.A., Tyack, P.L., 2004. Beaked whales echolocate on prey. Proc. R. Soc. B 271, S383–S386.
Johnston, D.W., McDonald, M., Polovina, J., Domokos, R., Wiggins, S., Hildebrand, J., 2008. Temporal patterns in the acoustic signals of beaked whales at Cross Seamount. Biol. Lett. 4, 208–211.
Kai, E.T., Rossi, V., Sudre, J., Weimerskirch, H., Lopez, C., et al., 2009. Top marine predators track Lagrangian coherent structures. PNAS 106, 8245–8250.
Kowarski, K.A., Delarue, J., Martin, B., O'Brien, J., Meade, R., et al., 2018. Signals from the deep: Spatial and temporal acoustic occurrence of beaked whales off western Ireland. PLoS One 13, e0199431.
Kowarski, K.A., Delarue, J.-J.-Y., Gaudet, B.J., Martin, S.B., 2021. Automatic data selection for validation: a method to determine cetacean occurrence in large acoustic data sets. JASA-EL 1, 051201.
Kowarski, K.A., Gaudet, B.J., Cole, A.J., Maxner, E.E., Turner, S.P., et al., 2020. Near real-time marine mammal monitoring from gliders: Practical challenges, system development, and management implications. J. Acoust. Soc. Am. 148, 1215–1230.
Kowarski, K.A., Martin, S.B., Maxner, E.E., Lawrence, C.B., Delarue, J.-J.-Y., Miksis-Olds, J.L., 2023. Cetacean acoustic occurrence on the US Atlantic Outer Continental Shelf from 2017 to 2020. Mar. Mamm. Sci. 39, 175–199.
Lazaridis E (2014) lunar: Lunar Phase & Distance, Seasons and Other Environmental Factors.
Lee, T.N., Yoder, J.A., Atkinson, L.P., 1991. Gulf Stream frontal eddy influence on productivity of the southeast U.S. continental shelf. J. Geophys. Res. Oceans 96, 22191–22205.
Lévy, M., Franks, P.J.S., Smith, K.S., 2018. The role of submesoscale currents in structuring marine ecosystems. Nat. Commun. 9, 4758.
MacLeod, C.D., Santos, M.B., Pierce, G.J., 2003. Review of Data on Diets of Beaked Whales: evidence of Niche Separation and Geographic Segregation. J. Mar. Biol. Assoc. U. K. 83, 651–665.
Mahadevan, A., 2019. Submesoscale Processes. In: Cochran, J.K., Bokuniewicz, H.J., Yager, P.L. (Eds.), Encyclopedia of Ocean Sciences, Third Edition. Academic Press, Oxford, pp. 35–41.
Malinka, C.E., Tønnesen, P., Dunn, C.A., Claridge, D.E., Gridley, T., Elwen, S.H., Madsen, P.T., 2021. Echolocation click parameters and biosonar behaviour of the dwarf sperm whale (Kogia sima). J. Exp. Biol. 224, jeb240689.
McCullough, J.L.K., Wren, J.L.K., Oleson, E.M., Allen, A.N., Siders, Z.A., Norris, E.S., 2021. An Acoustic Survey of Beaked Whales and Kogia spp. in the Mariana Archipelago using Drifting Recorders. Front. Mar. Sci. 8, 664292.
Merkens, K., Mann, D., Janik, V.M., Claridge, D., Hill, M., Oleson, E., 2018. Clicks of dwarf sperm whales (Kogia sima). Mar. Mamm. Sci. 34, 963–978.
Miksis-Olds, J., Ainslie, M.A., Butkiewicz, T., Clay, T.A., Hazen, E.L., et al., 2021. Atlantic Deepwater Ecosystem Observatory Network (ADEON): an integrated system for long-term monitoring of ecological and human factors on the Outer Continental Shelf (Synthesis report). U.S. Department of the Interior, Bureau of Ocean Energy Management.
Miksis-Olds, J.L., Ainslie, M.A., Blair, H.B., Butkiewicz, T., Hazen, E.L., et al., 2025. Overview of the Atlantic Deepwater Ecosystem Observatory Network Program. Oceanography 38, 40–51.
Miller, P., 2009. Composite front maps for improved visibility of dynamic sea-surface features on cloudy SeaWiFS and AVHRR data. J. Mar. Syst. 78, 327–336.
Miller, P.I., Scales, K.L., Ingram, S.N., Southall, E.J., Sims, D.W., 2015. Basking sharks and oceanographic fronts: quantifying associations in the north-east Atlantic. Funct. Ecol. 29, 1099–1109.
Mullaney, T.J., Suthers, I.M., 2013. Entrainment and retention of the coastal larval fish assemblage by a short-lived, submesoscale, frontal eddy of the East Australian current. Limnol. Oceanogr. 58, 1546–1556.
Owen, K., Andrews, R.D., Baird, R.W., Schorr, G.S., Webster, D.L., 2019. Lunar cycles influence the diving behavior and habitat use of short-finned pilot whales around the main hawaiian Islands. Mar. Ecol. Prog. Ser. 629, 193–206.
Prihartato, P.K., Irigoien, X., Genton, M.G., Kaartvedt, S., 2016. Global effects of moon phase on nocturnal acoustic scattering layers. Mar. Ecol. Prog. Ser. 544, 65–75.
Quick, N.J., Cioffi, W.R., Shearer, J.M., Fahlman, A., Read, A.J., 2020. Extreme diving in mammals: first estimates of behavioural aerobic dive limits in Cuvier's beaked whales. J. Exp. Biol. 223.
Rafter MA, Rice AC, Solsona Berga A, Frasier KE, Thayre BJ, et al. (2021) Passive Acoustic Monitoring for Marine Mammals Near Norfolk Canyon May 2019 – May 2020. Final Report. Marine Physical Laboratory Technical Memorandum 655. Submitted to Naval Facilities Engineering Systems Command (NAVFAC) Atlantic, Norfolk, Virginia, under Contract No. N62470-15-D-8006 Subcontract #3838476 (MSA2015-1176 Task Order 003) issued to HDR, Inc.
Rivière, P., Jaud, T., Siegelman, L., Klein, P., Cotté, C., Le Sommer, J., Dencausse, G., Guinet, C., 2019. Sub-mesoscale fronts modify elephant seals foraging behavior. Limnol. Oceanogr. Lett. 4, 193–204.
Roberts, J.J., Best, B.D., Mannocci, L., Fujioka, E., Halpin, P.N., et al., 2016. Habitat-based cetacean density models for the U.S. Atlantic and Gulf of Mexico. Sci. Rep. 6, 22615.
Roch, M.A., Brandes, T.S., Patel, B., Barkley, Y., Baumann-Pickering, S., Soldevilla, M.S., 2011. Automated extraction of odontocete whistle contours. J. Acoust. Soc. Am. 130, 2212–2223.
Rogers, A.D., Lavelle, A., Baird, R.W., Bender, A., Borroni, A., et al., 2024. A call to rename Ziphius cavirostris the goose-beaked whale: promoting inclusivity and diversity in marine mammalogy by re-examining common names. Mar. Mamm. Sci. 40, e13150.
Sabarros, P.S., Ménard, F., Lévénez, J.-J., Tew-Kai, E., Ternon, J.-F., 2009. Mesoscale eddies influence distribution and aggregation patterns of micronekton in the Mozambique Channel. Mar. Ecol. Prog. Ser. 395, 101–107.
Santos, M.B., Martin, V., Arbelo, M., Fernández, A., Pierce, G.J., 2007. Insights into the diet of beaked whales from the atypical mass stranding in the Canary Islands in September 2002. J. Mar. Biol. Assoc. U. K. 87, 243–251.
Savidge, D.K., Austin, J.A., 2007. The Hatteras Front: August 2004 velocity and density structure. J. Geophy. Res. 112.
Scales, K.L., Miller, P.I., Hawkes, L.A., Ingram, S.N., Sims, D.W., Votier, S.C., 2014a. On the Front Line: frontal zones as priority at-sea conservation areas for mobile marine vertebrates. J. Appl. Ecol. 51, 1575–1583.
Scales, K.L., Miller, P.I., Embling, C.B., Ingram, S.N., Pirotta, E., Votier, S.C., 2014b. Mesoscale fronts as foraging habitats: composite front mapping reveals oceanographic drivers of habitat use for a pelagic seabird. R. Soc. Open Sci. 11, 20140679.
Schorr, G.S., Falcone, E.A., Moretti, D.J., Andrews, R.D., 2014. First Long-Term Behavioral Records from Cuvier's Beaked Whales (Ziphius cavirostris) Reveal Record-breaking Dives. PLoS One 9, e92633.
Shearer, J.M., Quick, N.J., Cioffi, W.R., Baird, R.W., Webster, D.L., et al., 2019. Diving behaviour of Cuvier's beaked whales (Ziphius cavirostris) off Cape Hatteras, North Carolina. R. Soc. Open Sci. 6, 181728.
Simonis, A.E., Brownell, R.L., Thayre, B.J., Trickey, J.S., Oleson, E.M., et al., 2020. Co-occurrence of beaked whale strandings and naval sonar in the Mariana Islands. Western Pacific. Proc. r. Soc. b. 287, 20200070.
Simonis, A.E., Roch, M.A., Bailey, B., Barlow, J., Clemesha, R.E.S., et al., 2017. Lunar cycles affect common dolphin Delphinus delphis foraging in the Southern California Bight. Mar. Ecol. Prog. Ser. 577, 221–235.
Stanistreet, J.E., Nowacek, D.P., Baumann-Pickering, S., Bell, J.T., Cholewiak, D.M., et al., 2017. Using passive acoustic monitoring to document the distribution of beaked whale species in the western North Atlantic Ocean. Can. J. Fish. Aquat. Sci.
Tyack, P.L., Johnson, M., Soto, N.A., Sturlese, A., Madsen, P.T., 2006. Extreme diving of beaked whales. J. Exp. Biol. 209, 4238–4253.
Tyack, P.L., Zimmer, W.M.X., Moretti, D., Southall, B.L., Claridge, D.E., et al., 2011. Beaked Whales Respond to simulated and actual Navy Sonar. PLoS One 6, e17009.
Urmy, S.S., Benoit-Bird, K.J., 2021. Fear dynamically structures the ocean's pelagic zone. Curr. Biol. 31, 5086–5092.
van Rij J, Wieling, M., Baayen, R.H., van Rijn, H. (2022) itsadug: Interpreting Time Series and Autocorrelated Data Using GAMMs.
Virgili, A., Authier, M., Boisseau, O., Cañadas, A., Claridge, D., et al., 2019. Combining multiple visual surveys to model the habitat of deep-diving cetaceans at the basin scale. Glob. Ecol. Biogeogr. 28, 300–314.

Virgili, A., Hedon, L., Authier, M., Calmettes, B., Claridge, D., et al., 2021. Towards a better characterisation of deep-diving whales' distributions by using prey distribution model outputs? PLoS One 16, e0255667.
Visser, F., Merten, V.J., Bayer, T., Oudejans, M.G., de Jonge, D.S.W., et al., 2021. Deep-sea predator niche segregation revealed by combined cetacean biologging and eDNA analysis of cephalopod prey. Sci. Adv. 7, eabf5908.
Wang, B., Yu, F., Wang, R., Tao, Z., Ren, Q., et al., 2024. Intraseasonal variability of the deep scattering layer induced by mesoscale eddy. Front. Mar. Sci. 11, e30161.
Waring, G.T., Hamazaki, T., Sheehan, D., Wood, G., Baker, S., 2001. Characterization of Beaked Whale (Ziphiidae) and Sperm Whale (Physeter Macrocephalus) Summer Habitat in Shelf-Edge and deeper Waters off the Northeast U.S. Mar. Mamm. Sci. 17, 703–717.
West, K.L., Walker, W.A., Baird, R.W., White, W., Levine, G., et al., 2009. Diet of pygmy sperm whales (Kogia breviceps) in the hawaiian Archipelago. Mar. Mamm. Sci. 25, 931–943.
Wood S (2017) mgcv: Mixed GAM Computation Vehicle with Automatic Smoothness Estimation.
Ziegenhorn, M.A., Hildebrand, J.A., Oleson, E.M., Baird, R.W., Wiggins, S.M., Baumann-Pickering, S., 2023. Odontocete spatial patterns and temporal drivers of detection at sites in the hawaiian islands. Ecol. Evol. 13, e9688.
Zuur, A., Ieno, E.N., Walker, N., Saveliev, A.A., Smith, G.M., 2009. Mixed Effects Models and extensions in Ecology with R. Springer Science & Business Media.